

# Exclusion of non-crystalline polymer from the interlamellar region in polymer blends: poly(ether ether ketone)/poly(ether imide) blend by small-angle X-ray scattering

Chang Hyung Lee, Tetsuo Okada, Hiromu Saito and Takashi Inoue\*

Department of Organic and Polymeric Materials, Tokyo Institute of Technology, Ookayama, Meguro-ku, Tokyo 152, Japan

(Received 4 March 1996; accepted 18 March 1996)

Crystalline morphology in the blends of poly(ether ether ketone) (PEEK) and poly(ether imide) (PEI) was investigated by small-angle X-ray scattering. The lamellar thickness was found to be constant ( $\approx 6$  nm, independent of blend composition). The long period in 80/20 PEEK/PEI blend was greater than that in neat PEEK, whereas 50/50 PEEK/PEI blend showed intermediate value. This result suggests that a large amount of PEI impurity is excluded from interlamellar region in the high PEI content blend, whereas the exclusion is negligible and most PEI chains reside between lamellae in the low PEI content blend. The population of secondary lamellae, estimated by the interface distribution function analysis, was lowest in the 80/20 blend, suggesting that the formation of the secondary lamellae is restricted by the presence of the large amount of impurity between primary lamellae. Copyright © 1996 Elsevier Science Ltd.

(Keywords: blends; crystalline morphology; poly(ether ether ketone))

## INTRODUCTION

In miscible blend of crystalline and noncrystalline polymers, the noncrystalline impurity is excluded from crystallites. The degree of the exclusion may depend upon the relative rates ( $D/G$ ) of the diffusion rate of noncrystalline component ( $D$ ) and the growth rate of the crystalline component ( $G$ ). The exclusion is believed to occur in three ways<sup>1–3</sup>. If the value of  $D/G$  is comparable with the interlamellar distance, the noncrystalline component may reside at the interlamellar region. If  $D$  is larger (or  $G$  is smaller), the noncrystalline component resides between fibrils consisting of lamellar bundle. For very large  $D$  (or small  $G$ ),  $D/G$  may approach spherulitic dimension so that the noncrystalline component may be excluded outside of the spherulite. Because  $D$  is usually small in polymer/polymer systems, the noncrystalline polymer is expected to be excluded only on the length scale of lamellae or lamellar bundle.

Experimentally, the exclusion in a few micrometres could be characterized by optical microscope and that in a lamellae-scale by small-angle X-ray scattering (SAXS)<sup>3,4</sup>. For exclusion in an intermediate scale, small-angle light scattering is expedient. In a previous paper<sup>5</sup>, we investigated the crystallization kinetics of poly(ether ether ketone) (PEEK)/poly(ether imide) (PEI) blends by time-resolved light scattering. The correlation distance in orientation fluctuation  $\zeta$ , obtained by a Debye–Bueche plot for the angular dependence of  $H_v$  (cross-polarized) scattering intensity, increased with

increasing PEI content. The increase in  $\zeta$  was ascribed to the increase of distance between fibrils, which may be due to the excluded PEI from PEEK crystal lamellae. In this paper, we investigate the exclusion of PEI at the interlamellar region by SAXS.

## EXPERIMENTAL

We used commercial polymers: PEEK was VICTREX<sup>®</sup> from Mitsui Toatsu Chemicals, Inc. and PEI was ULTEM<sup>®</sup> 1000 from General Electric Co.

PEEK and PEI were melt-mixed at 380°C using Mini Max-Molder (CS-183MMX, Custom Scientific Instruments, Inc.) and then extruded. The extruded specimen was compression-moulded between metal plates at 380°C for 4 min. The moulded specimen was quenched to room temperature and then cut into thin strip (7 mm  $\times$  5 mm  $\times$  1 mm).

After the thin specimen was again melt on hot stage at 364°C for 3 min, it was rapidly transferred into a hot chamber set at 316°C and then isothermally crystallized for 12 h. The isothermally crystallized specimen was used for SAXS experiment. The X-ray beam was obtained from synchrotron radiation: beam line BL-10C at the National Laboratory for High Energy Physics, Tsukuba, Japan (Photon Factory)<sup>6</sup>.

The storage ring was operated at an energy level of 2.5 GeV with the ring current of 250–300 mA. The SAXS system employs point focusing optics with a double flat monochromator, followed by a bent cylindrical mirror. The incident beam intensity of 0.1488 nm wavelength was monitored by an ionization chamber for the

\* To whom correspondence should be addressed

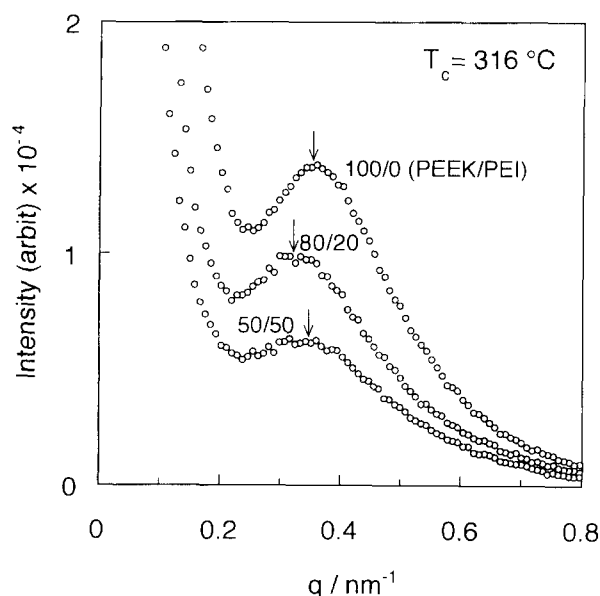


**Figure 1** SAXS profiles of PEEK, 80/20 blend and 50/50 blend; crystallized at 316°C for 12h

correction of minor decrease of the primary beam intensity during the measurement. The scattered intensity was detected with a one-dimensional position-sensitive proportional counter (PSPC) with 512 channels. The distance between the sample and the PSPC was about 2 m. The geometry was checked by using chicken tendon collagen, which gives a set of sharp diffraction corresponding to a Bragg spacing of 65.3 nm.

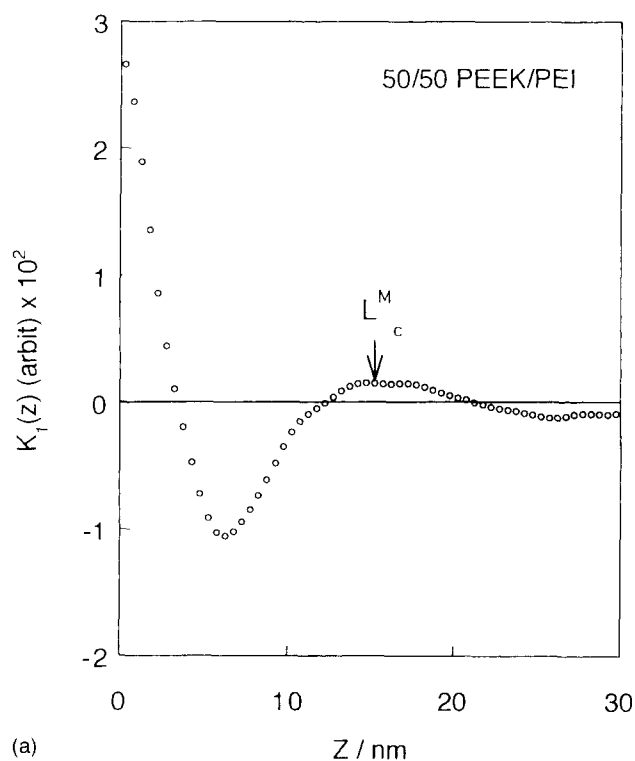
The scattering intensity  $I$  was corrected for background scattering. Then the scattering intensity by thermal fluctuations was subtracted from the SAXS profile  $I(q)$  by evaluating the slope of a  $I(q)q^4$  versus  $q^4$  plot<sup>7</sup> at wide scattering vectors  $q$ , where  $q$  is  $(4\pi/\lambda) \sin \theta$ ;  $\lambda$  and  $\theta$  being the wavelength and scattering angle of X-ray, respectively. The correction for smearing effect by the finite cross section of the incident beam was not necessary for the SAXS optics with point focusing.

## RESULTS AND DISCUSSION

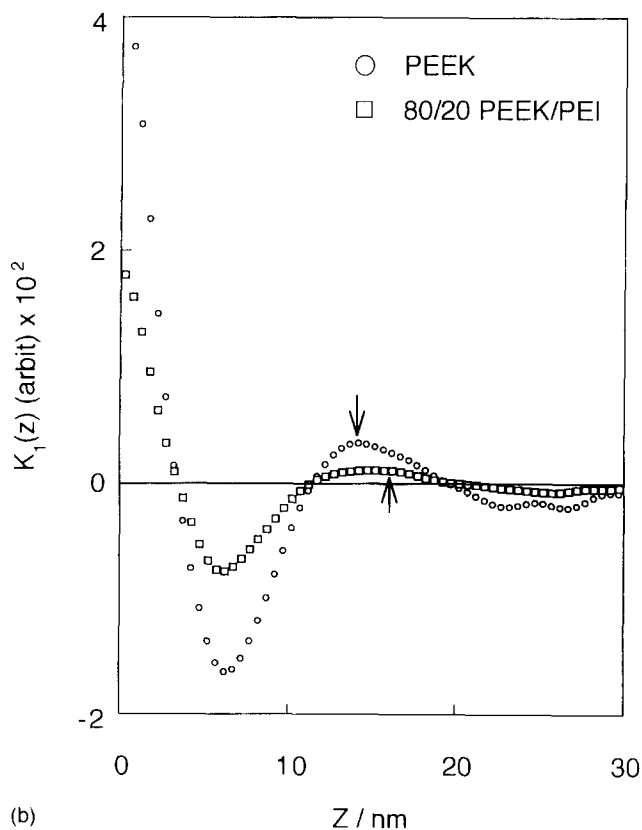
*Figure 1* shows the SAXS profiles. From the peak position of the SAXS profile, the long period  $L_B$  can be obtained by Bragg's law. Other parameters related to lamellar morphology can be estimated from the correlation function  $K_1(z)$ , which is given by the Fourier transform of the scattering intensity  $I(q)$ <sup>8</sup>:

$$K_1(z) = \int_0^\infty q^2 I(q) \cos(qz) dq \quad (1)$$

where  $z$  is the coordinate along which the electron density distribution is measured. The results of  $K_1(z)$  are shown in *Figure 2*. The long period  $L_c^M$  is determined by the position of the first maximum in the correlation function. Another important parameter is the lamellar thickness. The thickness may be calculated from the baseline procedure<sup>9</sup>, when the first minimum in the correlation function has a flat bottom. However, the bottom in *Figure 2* is not flat (as has been observed in many cases, the non-flat bottom is caused by the broad size distribution of the lamellae). One has then to use



(a)



(b)

**Figure 2** Correlation function: (a) 50/50 PEEK/PEI blend; (b) PEEK and 80/20 PEEK/PEI blend

another method. We employed the interface distribution function  $g_1(z)$  method because this is less affected by the superposition of the maxima or minima caused by the broad distribution rather than the shape of the correlation function<sup>10</sup>. The function  $g_1(z)$  is defined as

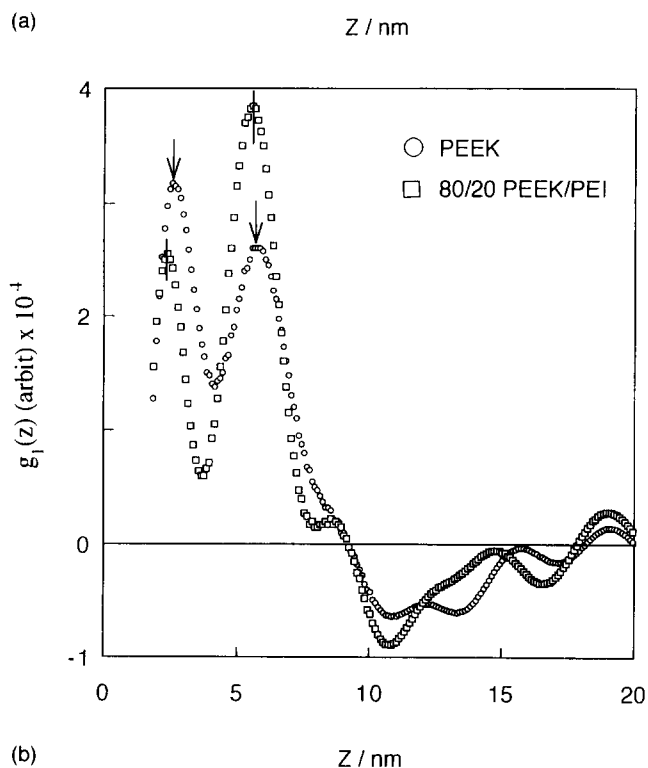
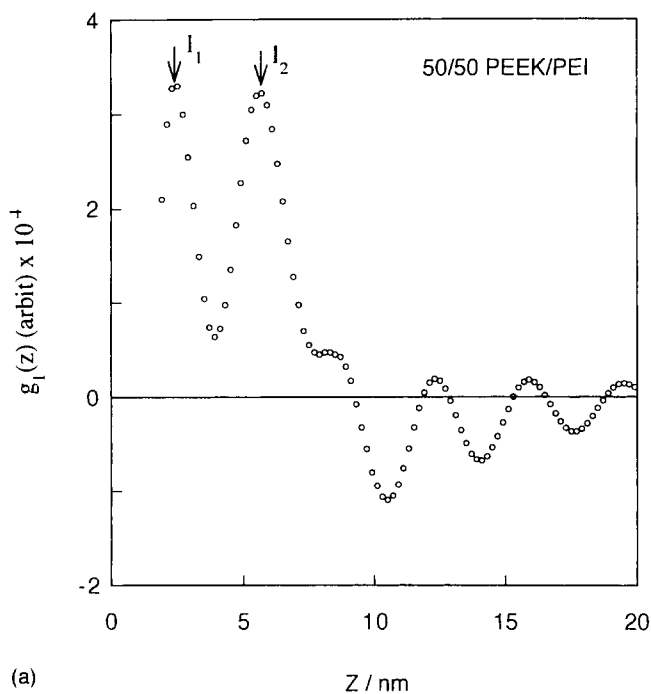


**Figure 3** Interface distribution function: (a) 50/50 PEEK/PEI blend; (b) PEEK and 80/20 PEEK/PEI blend

the second derivative of  $\gamma_1(z)$ :

$$g_1(z) = \gamma_1(z)'' \quad (4)$$

where  $\gamma_1(z)$  is the normalized one-dimensional correlation function defined by

$$\gamma_1(z) = \frac{1}{Q_{SAXS}} \int_0^{\infty} q^2 I(q) \cos(qz) dq \quad (5)$$

where  $Q_{SAXS}$  is the invariant of SAXS intensity. Results for  $g_1(z)$  are shown in Figure 3. Two peaks are seen, indicating the appearance of lamellae with two thicknesses. The thickness  $l_1$  is obtained from the position of

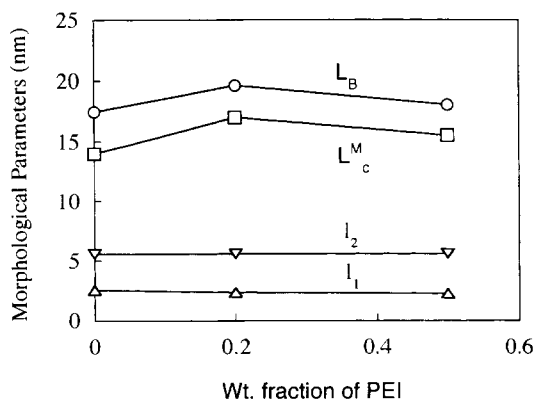


**Figure 4** Morphological parameters by SAXS as a function of blend composition:  $L_B$ , the long period by Bragg's law;  $L_c^M$ , the long period by the correlation function method;  $l_1$  and  $l_2$ , lamellar thickness by the interface distribution function method

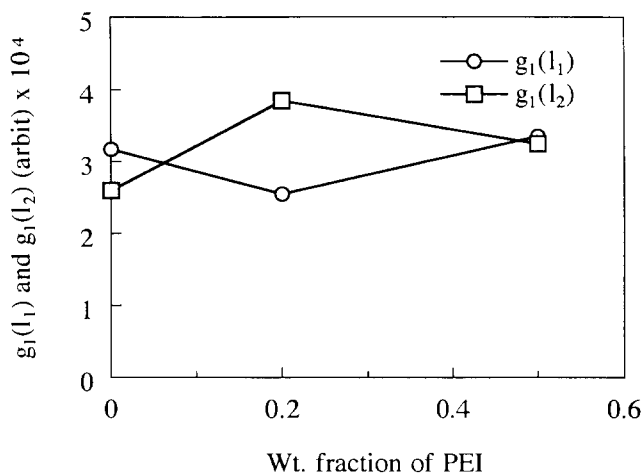


**Figure 5** Populations of thicker lamellae ( $l_2$ ) and thinner lamellae ( $l_1$ ) as a function of blend composition

the first maximum in  $g_1(z)$  and the thickness  $l_2$  by the second maximum. The thicker lamellae ( $l_2$ ) may be ascribed to the primary lamellae and the thinner ones ( $l_1$ ) to the secondary lamellae formed between the primary ones.

The morphological parameters by SAXS analyses are shown as a function of blend composition in Figure 4. The long period ( $L_B$  and  $L_c^M$ ) of the 80/20 PEEK/PEI blend is longer than that of neat PEEK. Taking account of constant lamellar thickness (independent of composition), this may suggest that a large amount of PEI is trapped between PEEK crystalline lamellae. In contrast, the long period of 80/20 PEEK/PEI blend is slightly larger than that of neat PEEK (and shorter than 80/20 blend), suggesting that a substantial amount of PEI should be excluded from interlamellar region.

Peak height  $g_1(l_i)$  in Figure 3 is a measure of population of lamellar crystal with thickness  $l_i$ . The values of  $g_1(l_1)$  and  $g_1(l_2)$  are plotted as a function of blend composition in Figure 5. The 80/20 PEEK/PEI blend shows largest  $g_1(l_1)$  and smallest  $g_1(l_2)$  values, which it may suggest that the presence of noncrystalline PEI between primary lamellae ( $l_2$ ) restricts the formation of secondary lamellae ( $l_1$ ). The 50/50 PEEK/PEI blend has almost the same populations of thick and thin lamellae, suggesting that the substantial exclusion of PEI provides less restriction for the formation of secondary lamellae.

## CONCLUSIONS

A series of morphological parameters by SAXS analyses, i.e., the long period, the lamellar thickness, the population of lamellae with different thicknesses, showed that a small amount of the impurity PEI is excluded from interlamellar region in the blend of low PEI content, whereas a substantial amount of the impurity PEI is excluded when PEI content is high.

## REFERENCES

- 1 Keith, H. D. and Padden Jr, F. J. *J. Appl. Phys.* 1963, **34**, 2409
- 2 Keith, H. D. and Padden Jr, F. J. *J. Appl. Phys.* 1964, **35**, 1270
- 3 Stein, R. S., Khambatta, F. B., Warner, F. P., Russell, T. P., Escala, A. and Balizer, E. *J. Polym. Sci., Polym. Symp.* 1978, **63**, 313
- 4 Saito, H. and Stühn, B. *Macromolecules* 1994, **27**, 216
- 5 Lee, C. H., Okada, T. and Inoue, T. *Kobunshi Ronbunshu* 1991, **48**, 581
- 6 Ueki, T., Hiragi, Y., Kataoka, M., Inoko, Y., Amemiya, Y., Izumi, T., Tagawa, H. and Muroga, Y. *Biophys. Chem.* 1985, **23**, 115
- 7 Koberstein, J. J., Morra, B. and Stein, R. S. *J. Appl. Crystallogr.* 1980, **13**, 34
- 8 Strobl, G. R. and Schneider, M. *J. Polym. Sci., Polym. Phys. Ed.* 1980, **18**, 1343
- 9 Strobl, G. R., Schneider, M. T. and Voigt-Martin I. G. *J. Polym. Sci., Polym. Phys. Ed.* 1980, **18**, 1361
- 10 Santa Cruz, C., Stribeck, N., Zachmann, H. G. and Balta Calleja, F. J. *Macromolecules* 1991, **24**, 5980